Bioinformatics analysis identifies ferroptosis-related genes in the regulatory mechanism of myocardial infarction

YONG-HAO JIANG[1], SU-YING WU[2], ZHEN WANG[1], LEI ZHANG[2], JUAN ZHANG[1], YAN LI[1], CHENGLONG LIU[2], WEN-ZHE WU[3] and YI-TAO XUE[1]

[1]Cardiovascular Department, Affiliated Hospital of Shandong University of Traditional Chinese Medicine; [2]Foreign Language College, Shandong University of Traditional Chinese Medicine, Jinan, Shandong 250000; [3]Cardiovascular Department, Dezhou Municipal Hospital, Dezhou, Shandong 253000, P.R. China

Received July 11, 2022; Accepted September 22, 2022

DOI: 10.3892/etm.2022.11684

Abstract. Since ferroptosis is considered to be a notable cause of cardiomyocyte death, inhibiting ferroptosis has become a novel strategy in reducing cardiac cell death and improving cardiopathic conditions. Therefore, the aim of the present study was to search for ferroptosis-related hub genes and determine their diagnostic value in myocardial infarction (MI) to aid in the diagnosis and treatment of the disease. A total of 10,286 DEGs were identified, including 6,822 upregulated and 3.464 downregulated genes in patients with MI compared with healthy controls. After overlapping with ferroptosis-related genes, 128 ferroptosis-related DEGs were obtained. WGCNA successfully identified a further eight functional modules, from which the blue module had the strongest correlation with MI. Blue module genes and ferroptosis-related differentially expressed genes were overlapped to obtain 20 ferroptosis-related genes associated with MI. Go and KEGG analysis showed that these genes were mainly enriched in cellular response to chemical stress, trans complex, transferring, phosphorus-containing groups, protein serine/threonine kinase activity, FoxO signaling pathway. Hub genes were obtained from 20 ferroptosis-related genes through the PPI network. The expression of hub genes was found to be down-regulated in the MI group. Finally, the miRNAs-hub genes and TFs-hub genes networks were constructed. The GSE141512 dataset and the use of RT-qPCR assays on patient blood samples were used to confirm these results. The results showed that ATM, PIK3CA, MAPK8, KRAS and SIRT1 may play key roles in the development of MI, and could therefore be novel markers or targets for the diagnosis or treatment of MI.

Correspondence to: Professor Wen-Zhe Wu, Cardiovascular Department, Dezhou Municipal Hospital, 1766 Sanba Zhong Road, Decheng, Dezhou, Shandong 253000, P.R. China
E-mail: 1186046188@qq.com

Professor Yi-Tao Xue, Cardiovascular Department, Affiliated Hospital of Shandong University of Traditional Chinese Medicine, 16369 Jingshi Road, Jinan, Shandong 250000, P.R. China
E-mail: xytsdzyy@126.com

Key words: myocardial infarction, ferroptosis, weighted gene co-expression network analysis, diagnosis, biomarker

Introduction

Myocardial infarction (MI) is a severe disease that occurs globally; from 2002 to 2015, the incidence of MI was ~242/100,000 individuals per year (1). According to the universal definition of MI (2), it may be divided into five types and is primarily induced by acute myocardial ischemia resulting from several factors. For example, the rupture of acute atherosclerotic plaques leads to ischemic myocardial damage due to the mismatch between oxygen supply and demand (3). Based on the existing clinical guidelines (4,5), clearing blocked vessels and reducing thrombotic obstruction with drugs as quickly as possible are the two most important treatment options. However, for vessels that are difficult to clear and when MI is caused by microvascular lesions, only conservative drug treatment should be used and recurrent attacks are more probable (6). Consequently, it is important to identify novel therapeutic targets to reduce MI.

Ferroptosis is a process in which unsaturated fatty acids are highly expressed on the cell membrane and are subject to lipid peroxidation by Fe^{2+} ions and lipoxygenase, thereby inducing cell death. It is also hallmarked by a decrease in the expression of the glutathione-dependent antioxidant system and glutathione peroxidase 4 (GPX4) enzymes (7). Ferroptosis is involved in tumor cell death, neurodegenerative diseases, renal failure and cardiac ischemic injury (8-10). MI is a severe type of ischemic heart disease in which ferroptosis plays a central role (11). At present, studies on the mechanism of ferroptosis in MI have primarily focused on endoplasmic reticulum stress, reactive oxygen species (ROS) generation, GPX4 and the autophagy-dependent ferroptosis pathway (11-15). Several studies have concluded that the inhibition of cardiomyocyte ferroptosis is a potentially important target for MI treatment. For example, treatment of an MI mouse model using ferrostatin-1 (an inhibitor of ferroptosis) or dexrazoxane (an iron-chelating agent) can reduce MI scar areas and myocardial enzyme activity (16). In addition, baicalin has been shown to prevent MI by inhibiting long-chain-fatty-acid-CoA ligase

4-mediated ferroptosis (17). Moreover, other drugs, such as piperonylamine and artesunate, have also inhibited ferroptosis and represent potential drugs for the treatment of related diseases (18,19).

Since ferroptosis plays a key role in MI, in the present study genes associated with MI and ferroptosis were identified. These genes may be useful for identifying putative therapeutic targets or providing a theoretical basis for understanding the molecular pathology of MI. Furthermore, microRNAs (miRNAs/miRs), transcription factors (TFs) and targeted drugs were analyzed in context to the above genes, and differential expression of these genes was verified using a separate dataset and clinical specimens. The present study provides a basis for further research exploring the potential therapeutic targets and regulatory mechanisms of MI, and also provides a new treatment strategy.

Materials and methods

Data sources. The transcriptome data of the current study were obtained from two datasets, GSE59867 (20) and GSE141512 (21) datasets of Gene Expression Omnibus (GEO) database (http://www.ncbi.nlm.nih.gov/geo/) (22). The population of the GSE59867 dataset consisted of 46 controls and 390 MI samples, and was used as a training set. The GSE141512 dataset consisted of 6 controls and 6 MI samples, and was used as an external validation set. The ferroptosis-related genes were extracted from the FerrDb database (http://www.zhounan.org/ferrdb). After removing the duplicated genes of the three subgroups of ferroptosis gene sets, a total of 259 genes were obtained (23).

Acquisition of differentially expressed genes (DEGs). All the microarray data after normalization were analyzed by R 4.1.0 software (24). The R package, 'limma', was used to identify differentially expressed mRNAs between MI and control samples, with adjusted P-value <0.05 as the threshold (25). A heatmap cluster and volcano plot of the DEGs were created using the 'ggplot2' packages via R software. Furthermore, by intersecting with ferroptosis-related genes, the ferroptosis-related DEGs were obtained and the heat map of ferroptosis-related DEGs was created using the 'pheatmap' package (26).

Gene set enrichment analysis (GSEA). The potential biological function of the DEGs was enriched using the GSEA method and annotated using Gene Ontology (GO) (http://geneontology.org/) and Kyoto Encyclopedia of Genes and Genomes (KEGG) databases (https://www.kegg.jp/). In GSEA, a false discovery rate (FDR) of <0.05 was considered to indicate DEGs that were significantly enriched.

Weighted gene co-expression network analysis (WGCNA). The GEO expression file was used for WGCNA using the WGCNA R package (27). Firstly, samples were clustered to assess the presence of any outliers. Then, the automatic network construction function was used to obtain the co-expression network. The 'pick Soft Threshold' function was used (set to 15) to calculate the soft thresholding power β. Furthermore, the matrix data were then transformed into an adjacency matrix, hierarchical clustering and the 'dynamic Tree Cut' function were used to detect modules. After completing the calculation of module eigengene (ME) and merging similar modules in the clustering tree according to ME, a hierarchical clustering dendrogram was drawn. Modules were combined with phenotypic data to calculate gene significance (GS) and module significance (MS) to measure the significance of genes and clinical information and analyze the correlation between modules and clinical features. Then which modules are most relevant to MI was revealed.

Functional annotation and pathway enrichment analysis. To reveal the functions of DEGs, GO annotation (28) and KEGG enrichment (29) analysis were conducted using the 'cluster profile' package. GO enrichment results of 'biological process' (BP), 'cellular component' (CC) and 'molecular function' (MF) were obtained. KEGG pathway analysis was used to describe gene function at the genomic and molecular levels and reveal the associated genes. $P<0.05$ was considered to indicate a statistically significant difference.

Protein-protein interaction (PPI) network construction. The PPI network was constructed using the STRING database (30). The confidence score was set at 0.4 for the PPI analysis and was considered statistically significant. Cytoscape 3.8.2 was used to visualize the PPI network (31). Cytoscape plugin, MCODE, was used to screen the significant modules in the PPI network.

Validation of hub genes. Receiver operating characteristic (ROC) curve analysis was performed using the pROC package (32) to evaluate the diagnostic value of the hub genes for MI. ROC curve analysis, which yields indictors of accuracy, such as the area under the curve (AUC), provides the basic principle and rationale for distinguishing between the specificity and sensitivity of diagnostic performance.

Analysis of interaction effect and functional similarity for hub genes. The 'ggpubr' package was used to perform Spearman's correlation analysis on hub genes. The 'ggpubr' was a flexible package for data visualization based on 'ggplot2' package in R (33). Moreover, the functional similarity among proteins was evaluated using the geometric mean of semantic similarities in CCs and MFs through the GOSemSim package (34). Functional similarity measures the strength of the relationship between each protein and its partners by considering the function and location of proteins.

Construction of gene-drug interaction network and regulatory network of hub genes . In order to explore the potential therapeutic drugs for MI, DEGs were uploaded to the CMAP database (https: //www.complement.us/cmap) (34), and relevant drugs associated with MI treatment were identified. Then, drugs targeting proteins encoded by hub genes were identified using the through the Comparative Toxicogenomics Database (CTD) (35). MiRNet database (36) was used to predict the TFs and miRNAs of hub genes. Hub genes and their TFs and miRNAs were integrated into a regulatory network, and visualized using Cytoscape software.

Sample collection. The present study was approved by the Ethics Committee of Dezhou Municipal Hospital (Dezhou,

China; approval no. 2022-L-06; January 17, 2022) and complied with The Declaration of Helsinki. Written informed consent was obtained from all subjects. A total of 5 patients with MI and 5 patients with stable angina pectoris/chronic coronary syndromes (CCS) were enrolled at Dezhou Municipal Hospital (Dezhou, China) between February 2022 and March 2022, and blood draws were completed at the hospital. The diagnoses of the patients followed the latest diagnostic guidelines. The diagnosis of MI was in accordance with the Fourth Universal Definition of Myocardial Infarction (2018) (3). MI is diagnosed when there is clinical evidence of acute myocardial ischemia and the rise or fall of cardiac troponin T values with at least one value exceeding the 99th percentile upper reference limit, followed by at least one of the following: i) Symptoms of myocardial ischemia; ii) changes on an electrocardiogram indicating new ischemia; iii) development of pathological Q waves on an electrocardiogram; iv) new loss of viable myocardium or new regional wall motion abnormality evidenced by imaging; and v) coronary thrombus evidenced by angiography or autopsy. CCS is diagnosed when the following three characteristics are met simultaneously: i) Retrosternal discomfort (its nature and duration have typical characteristics) (37); ii) fatigue or emotional stress can be induced; and iii) rest or nitrates can provide relief. The above criteria were met, and serum cardiac troponin I (cTnI) and myocardial enzymes were negative (38,39). Subjects diagnosed with CCS were considered to be the control group. Peripheral blood collection was completed within 12 h after admission.

Inclusion criteria: i) Patients met the diagnostic criteria for MI or CCS; ii) patients were aged between 40-80 years old (sex was not limited); and iii) patient hemodynamics were stable, and there was no evident abnormality in liver and kidney function.

Exclusion criteria: i) Patients with acute decompensation of chronic heart failure, symptomatic hypotension (systolic blood pressure <90 mmHg) or an expected survival period of <3 months; ii) patients with abnormal liver and kidney function and serious primary disease (for example, acute exacerbation of chronic obstructive pulmonary disease, diabetic ketoacidosis, multiple tumor metastasis); iii) pregnant and lactating women; iv) patients who have previously been found to be allergic to the experimental drug; or v) the presence of factors that can increase death, such as severe arrhythmia, pulmonary embolism, cardiogenic shock or obvious infection.

RNA extraction and reverse transcription-quantitative PCR (RT-qPCR). Total RNA from peripheral blood was extracted using the SPEAKeasy Serum/Plasma RNA kit (Shandong Sparkjade Biotechnology Co., Ltd.) according to the manufacturer's protocol under low temperature. The Nano400 Spectrophotometer (Hangzhou Allsheng Instruments Co., Ltd.) was utilized to check the concentration and purity of the extracted RNA, with the A260/A280 ratio between 1.8 and 2.0. cDNA synthesis was conducted using HiScript II Q RT SuperMix (Vazyme Biotech Co., Ltd.) according to the manufacturer's protocol. Using GAPDH as a reference, RT-qPCR was performed with ChamQ Universal SYBR qPCR Master Mix (cat. no. R311-02; Vazyme Biotech Co., Ltd.) in the CFX96 Touch Real-Time PCR Detection System (Bio-Rad Laboratories, Inc.). Primer sequences (TsingKe Biological Technology) for reference and candidate genes are shown in Table I. The thermocycling protocol for PCR was as follows: 50˚C For 3 min, 95˚C for 2 min, followed by 40 cycles of 95˚C for 10 sec and 60˚C for 10 sec. The $2^{-\Delta\Delta Cq}$ method was applied to calculate the relative expression level of mRNA (40).

Table I. Primer sequences for reverse transcription-quantitative PCR.

Gene	Direction	Primer sequence (5'-3')
ATM	Forward	GGAGCCATAATTCAGGGTAGT
	Reverse	GTCAGTGCCAAAGTCAAACA
KRAS	Forward	TGGCGTAGGCAAGAGTG
	Reverse	TTGACCTGCTGTGTCGAG
PIK3CA	Forward	GACGCATTTCCACAGCTAC
	Reverse	CACATAAGGGTTCTCCTCCA
MAPK8	Forward	TCTCCAACACCCGTACATC
	Reverse	CCTCCAAGTCCATAACTTCCT
SIRT1	Forward	TTCCAGCCATCTCTCTGTC
	Reverse	ATTCCCGCAACCTGTTC
GAPDH	Forward	CCTTCCGTGTCCCCACT
	Reverse	GCCTGCTTCACCACCTTC

Statistical analysis. SAS 9.4 (SAS Institute, Inc.) was used to analyze the clinical data, and the measurement data were tested for normality first. Two groups were compared using independent Student's t-test. If non-conformity was expressed as the median (Q1-Q3), Wilcoxon rank-sum test was used. Enumeration data were compared between the two groups using the x^2 test. If the theoretical frequency was too small, Fisher's exact probability method was used. All experiments were performed three times, and the results are expressed as the mean ± standard error of the mean. GraphPad Prism 9 (GraphPad Software, Inc.) was used to analyze the data. The statistically significant differences between the MI group and controls were examined using independent Student's t-test. $P<0.05$ was considered to indicate a statistically significant difference.

Results

Identification of DEGs. After standardization of the microarray results from GSE59867, a total of 10,286 DEGs, including 6,822 upregulated genes and 3,464 downregulated genes, were detected, as shown in Fig. 1. GSEA analysis showed that upregulated genes were enriched in GO and KEGG pathways, including 'Glycolysis gluconeogenesis', 'Myeloid leukocyte mediated immunity', 'Tertiary granule' and 'Cargo receptor activity'. Downregulated genes were enriched in 'Cell cycle', 'mRNA processing', 'Ribonucleoprotein complex' and 'ATPase activity' (Fig. 2A-D).

Analysis of ferroptosis-related DEGs. A total of 259 ferroptosis-related genes were extracted from the FerrDb database. After intersecting them with the DEGs, a total of 128 ferroptosis-related DEGs were found. The Venn diagram of the ferroptosis-related DEGs are shown in Fig. 3A. Fig. 3B,

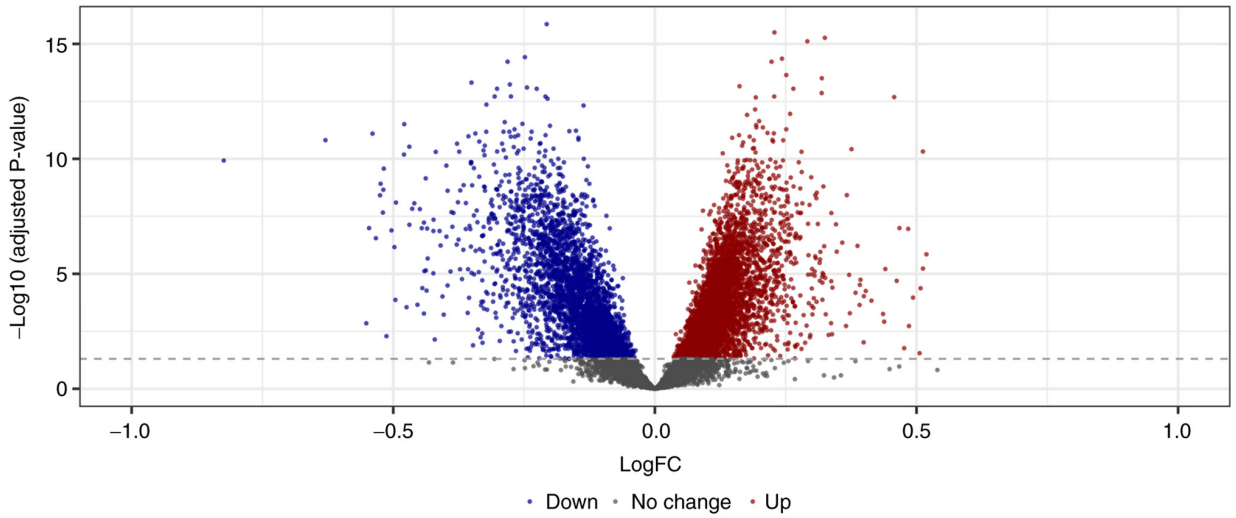

Figure 1. Volcano plot for the analysis of the differentially expressed genes. FC, fold change.

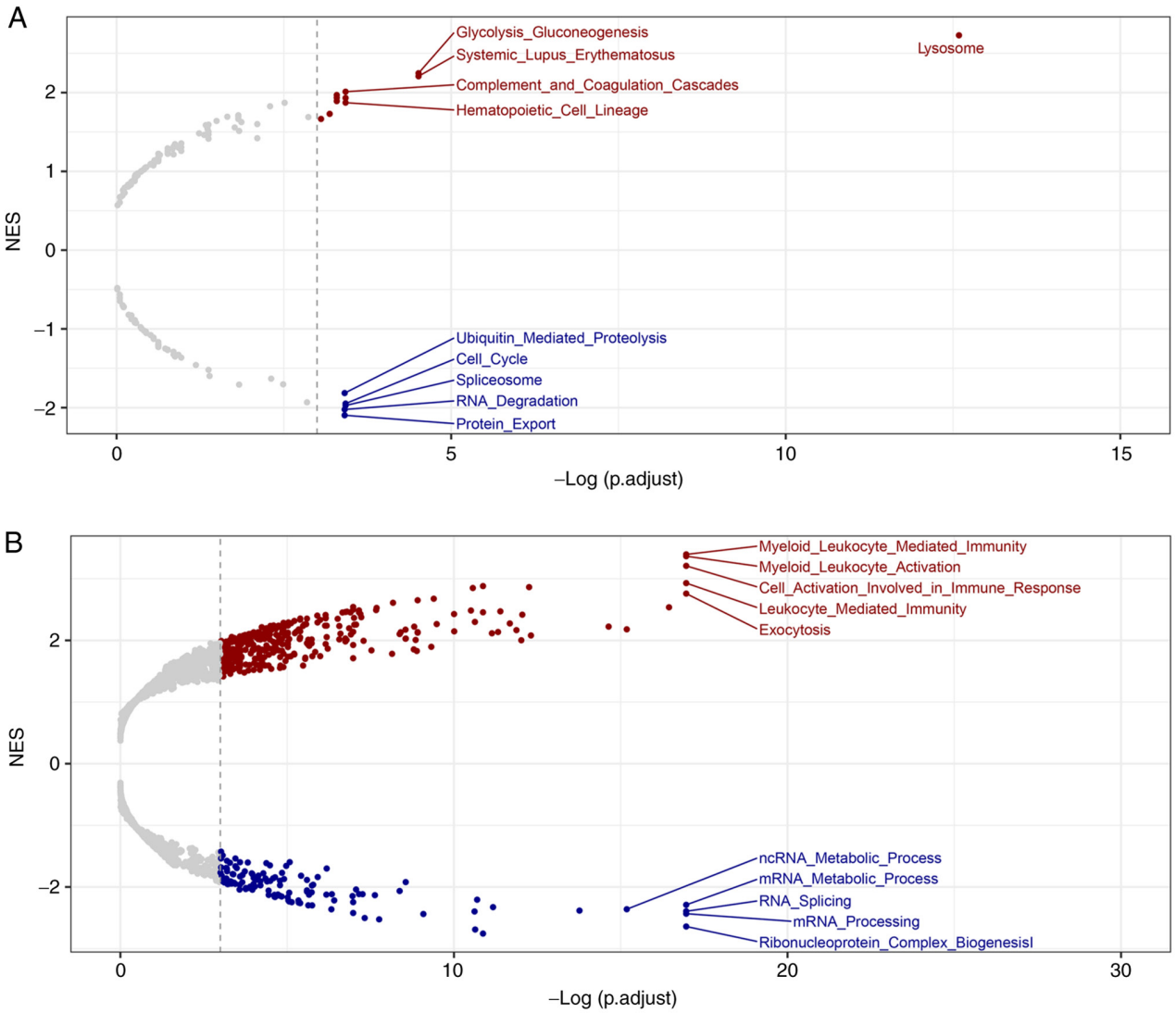

Figure 2. Continued

which presents the 10 most significantly upregulated and 10 downregulated genes by heat map, indicating the differential expression of ferroptosis-related DEGs between the control and MI groups.

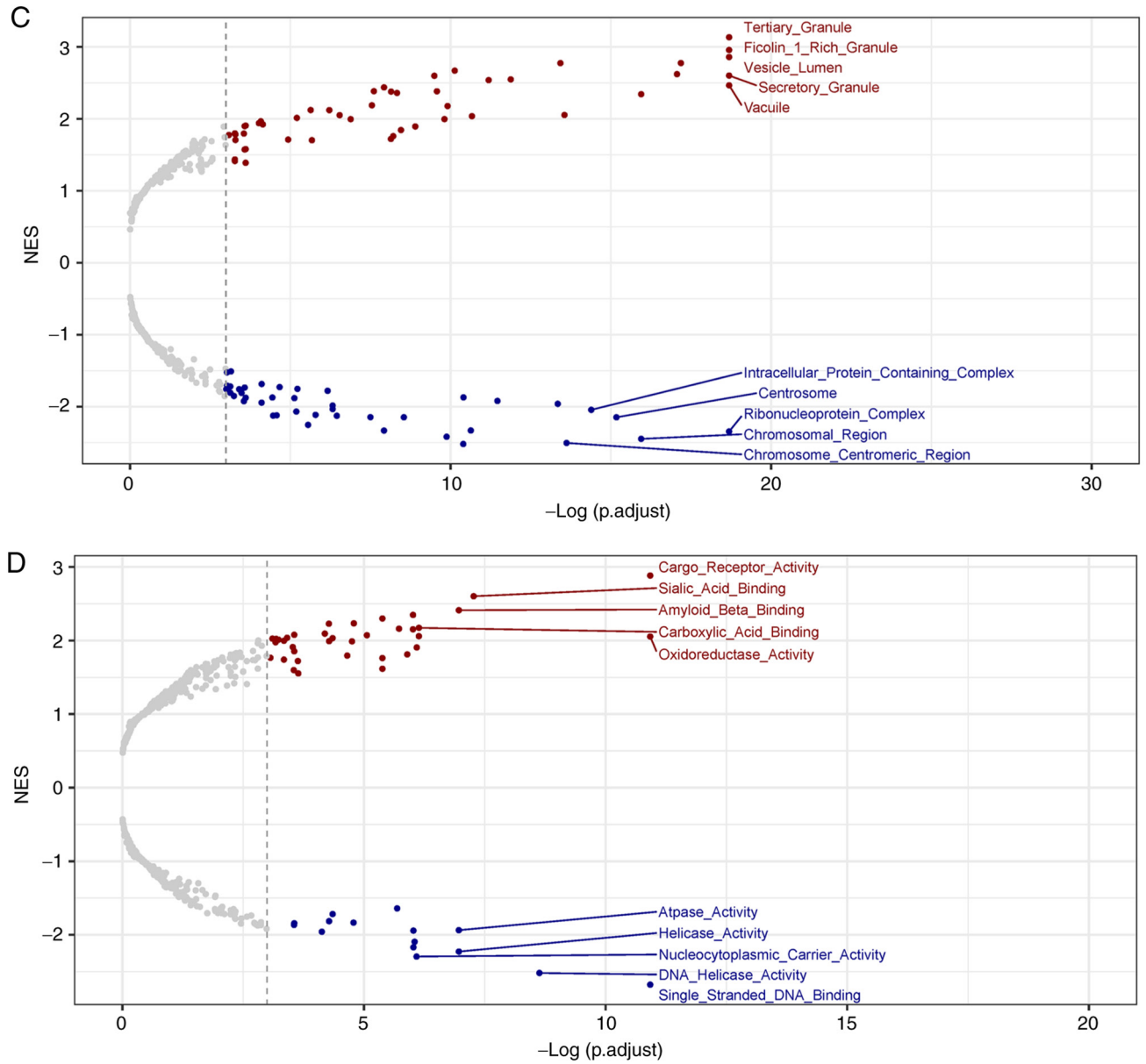

Figure 2. Gene set enrichment analysis for the differentially expressed genes. (A) Kyoto Encyclopedia of Genes and Genomes pathways. (B) GO for 'biological process'. (C) GO for 'cellular component'. (D) GO for 'molecular function'. GO, Gene Ontology; NES, Normalized Enrichment Score.

Weighted co-expression network construction and identification of key modules. Euclidean distance of the expression was used to perform hierarchical clustering. There were no outliers to remove (Fig. 4A). The soft threshold was set to 15 to construct a scale-free network (Fig. 4B). Next, eight modules were identified based on average hierarchical clustering and dynamic tree clipping (Fig. 4C). The blue module was the most relevant module associated with MI (Fig. 4D). Thus, a total of 1,547 genes in this module were selected for further analysis.

GO and KEGG enrichment analysis of ferroptosis-related genes. Blue module genes and ferroptosis-related DEGs were overlapped to obtain 20 ferroptosis-related genes (Fig. 5). The 20 genes are TGFBR1, ZEB1, SNX4, IREB2, ATG5, KRAS, SLC38A1, FANCD2, ATM, MAPK8, MAP3K5, FBXW7, MAPK9, EMC2, PIK3CA, SIRT1, KLHL24, OXSR1, GABPB1 and PRKAA1. It was observed that for GO-BP they were mainly enriched in 'cellular response to chemical stress', 'response to oxidative stress' and 'cellular response to oxidative stress' (Fig. 6A). For GO-CC, the genes were mainly enriched in 'transferase complex, transferring phosphorus-containing groups' and 'protein kinase complex' (Fig. 6B). Finally, regarding GO-MF, the genes were mainly enriched in 'protein serine/threonine kinase activity' ,'protein serin kinase activity' and 'protein threonine kinase activity' (Fig. 6C). Moreover, KEGG analysis revealed that those genes were mainly involved in the 'FoxO signaling pathway', 'Longevity regulating pathway-multiple species' and 'Apoptosis' (Fig. 6D).

PPI network construction and module analysis. To further study the interaction of the 20 ferroptosis-related genes, a PPI network was constructed using the STRING database. A total

Figure 3. Ferroptosis related DEGs. (A) Venn diagram showing the overlap between the DEGs and ferroptosis-related genes. (B) Heatmap for ferroptosis-related DEGs in patients with MI and controls. DEG, differentially expressed gene; MI, myocardial infarction.

of six of the 20 genes were not related to other molecules and did not form a molecular network. With a confidence of >0.4 and hiding the disconnected nodes, a visualized PPI network was created using Cytoscape (Fig. 7A). Using the MCODE plugin, five genes in the key module were selected as hub genes, namely ATM, PIK3CA, MAPK8, KRAS and SIRT1 (Fig. 7B).

Analysis of interaction effect and functional similarity of hub genes. Analysis of the interactome of the hub genes revealed that ATM and PIK3CA had the highest correlation (Fig. 8A). Proteins were ranked by their average functional similarity relationships among proteins within the interactome. ATM, MAPK8 and PIK3CA were the three top-ranked proteins potentially playing key roles in MI (Fig. 8B).

Multi-factor regulation network construction. Based on the results from miRNet database, miRNAs-hub gene (Fig. 9A) and TFs-hub gene (Fig. 9B) networks were constructed using Cytoscape software. In order to facilitate the selection of key miRNAs, miRNAs targeting ≥3 hub genes were selected for network analysis. Finally, the network included five hub genes, 43 miRNAs and 34 TFs.

Drug prediction. The Connectivity Map (CMap) database was used to search for potential drugs associated with MI (41,42). Based on the interaction information of genes and drugs in the CTD database, the association between potential drugs and hub genes was obtained Among them, dorsomorphin is a small-molecule drug may act on five hub genes (Fig. 10).

Evaluation of the diagnostic performance of hub genes in GSE59867. The expression of hub genes in MI and control samples was detected, and it was found that the expression of hub genes was downregulated in MI (Fig. 11A). The diagnostic values of hub genes were further evaluated by ROC curves. It was found that ATM, PIK3CA and MAPK8 had high accuracy with AUC values of >0.7 (Fig. 11B).

Expression of hub genes in GSE141512. The expression of hub genes was verified in the GSE141512 dataset, and it was found that the expression of all hub genes was downregulated in the MI group compared with the control. ATM, PIK3CA and SIRT1 genes showed significant differences in the expression between the MI and control groups (Fig. 12).

Baseline characteristics of study subjects. In patients with CCS, there is no necrosis of the myocardium. Therefore, the CCS group was used as the normal control group. Moreover, the basic conditions between the MI and CCS groups, such as age, past medical history and medication history, were similar. A total of 10 participants were recruited in the present study

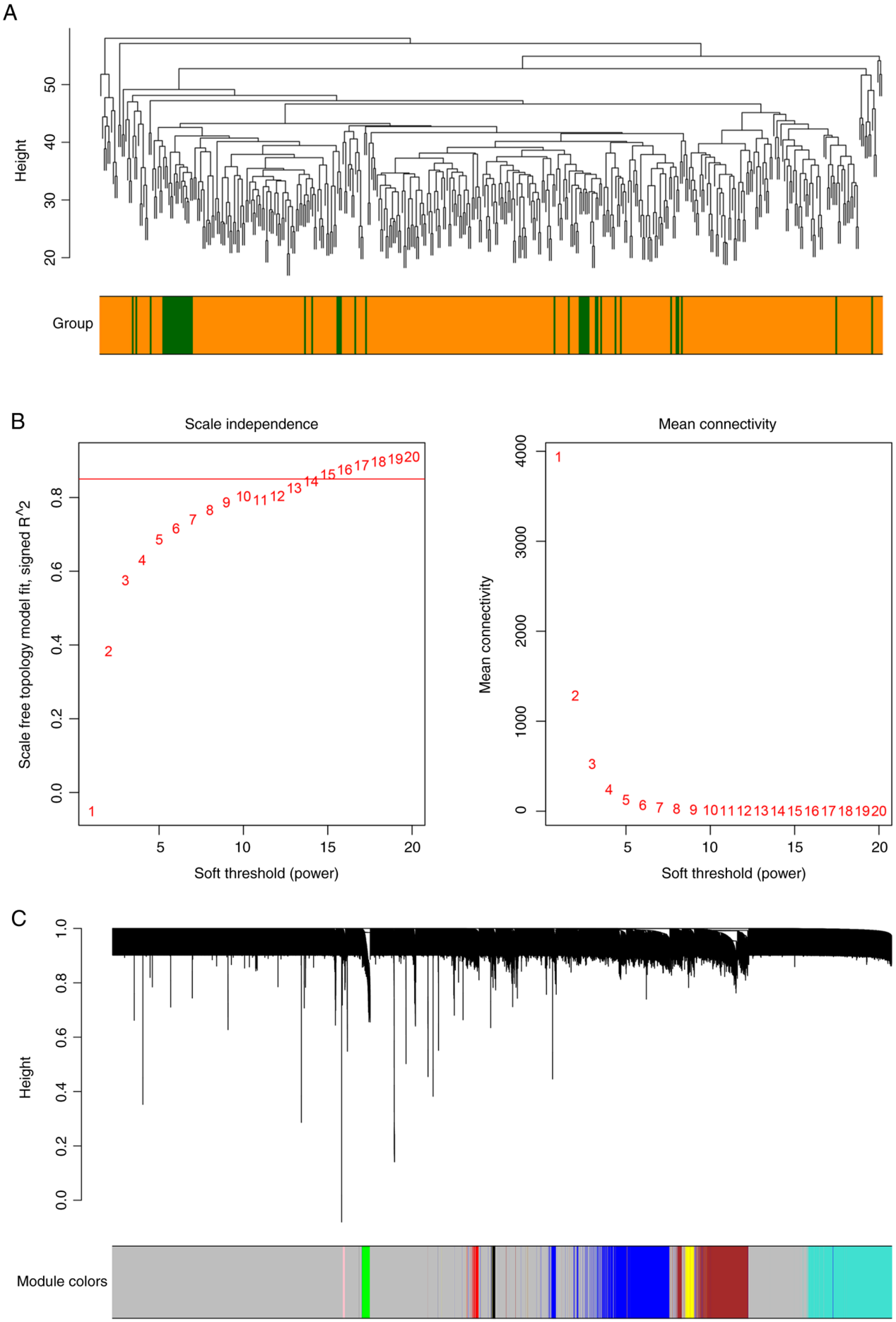

Figure 4. Continued.

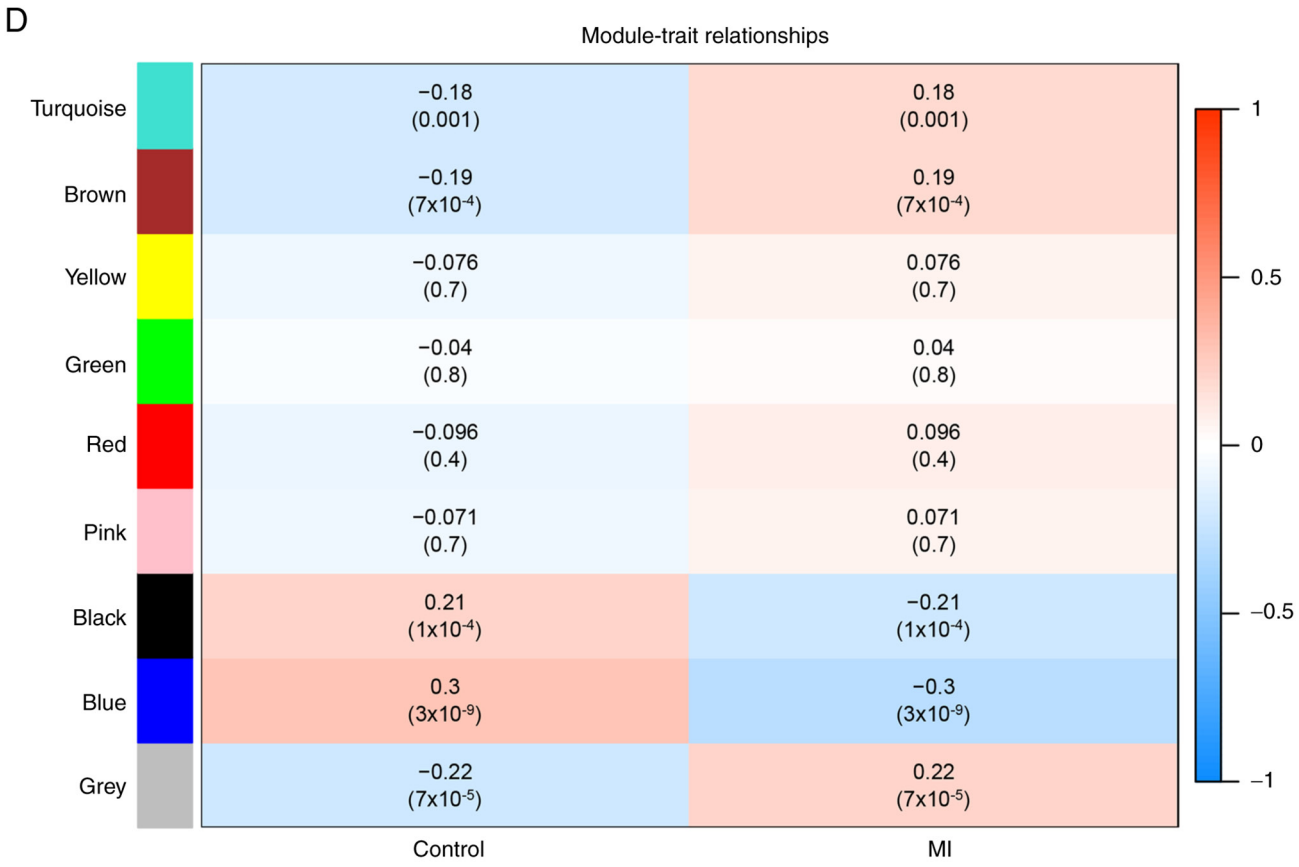

Figure 4. Weighted co-expression network construction and identification of key modules. (A) Sample clustering to detect outliers. (B) Soft threshold selection. (C) Co-expression modules selection. (D) Correlation between co-expression modules and MI. MI, myocardial infarction.

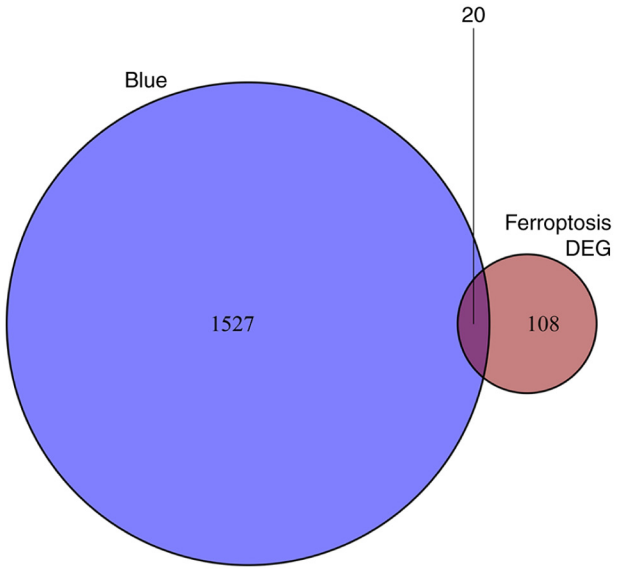

Figure 5. Venn diagram showing the co-expression of ferroptosis-related DEGs. DEG, differentially expressed gene.

and were separated into two groups, MI (n=5) and controls (n=5). Comparison between groups showed that the levels of high-sensitivity cTnI, creatine kinase-MB and low-density lipoprotein-cholesterol were statistically different between the two groups (P<0.05). The demographic, clinical features, medication history and laboratory data of all participants are shown in Table II.

Validation of the hub genes. RT-qPCR was used to detect the transcriptional changes of all overlapped hub genes in peripheral blood from the controls and patients with MI. The results indicated that the expression levels of all hub genes were decreased in the MI group in comparison with those in controls (Fig. 13).

Discussion

In the current study, five hub genes associated with ferroptosis in patients with MI were screened by comprehensive bioinformatics analysis, namely ATM, KRAS, MAPK8, PI3KCA and SIRT1. miRNAs and transcription factors targeting the hub genes were selected to construct the corresponding regulatory network, as well as potential therapeutic drugs for MI targeting of the hub genes. Subsequently, using the GSE141512 validation set, the five hub genes were all confirmed as lowly-expressed genes in the MI group. Of these, the inter-group differences of ATM, PI3KCA and SIRT1 were statistically significant. Finally, it was verified that gene expression was decreased in patients with MI and CCS.

GSEA enrichment analysis was also performed for the 10,286 identified DEGs. The intersection of DEGs and ferroptosis-related genes revealed 128 ferroptosis-related DEGs. Intersecting with the candidate genes for MI screened

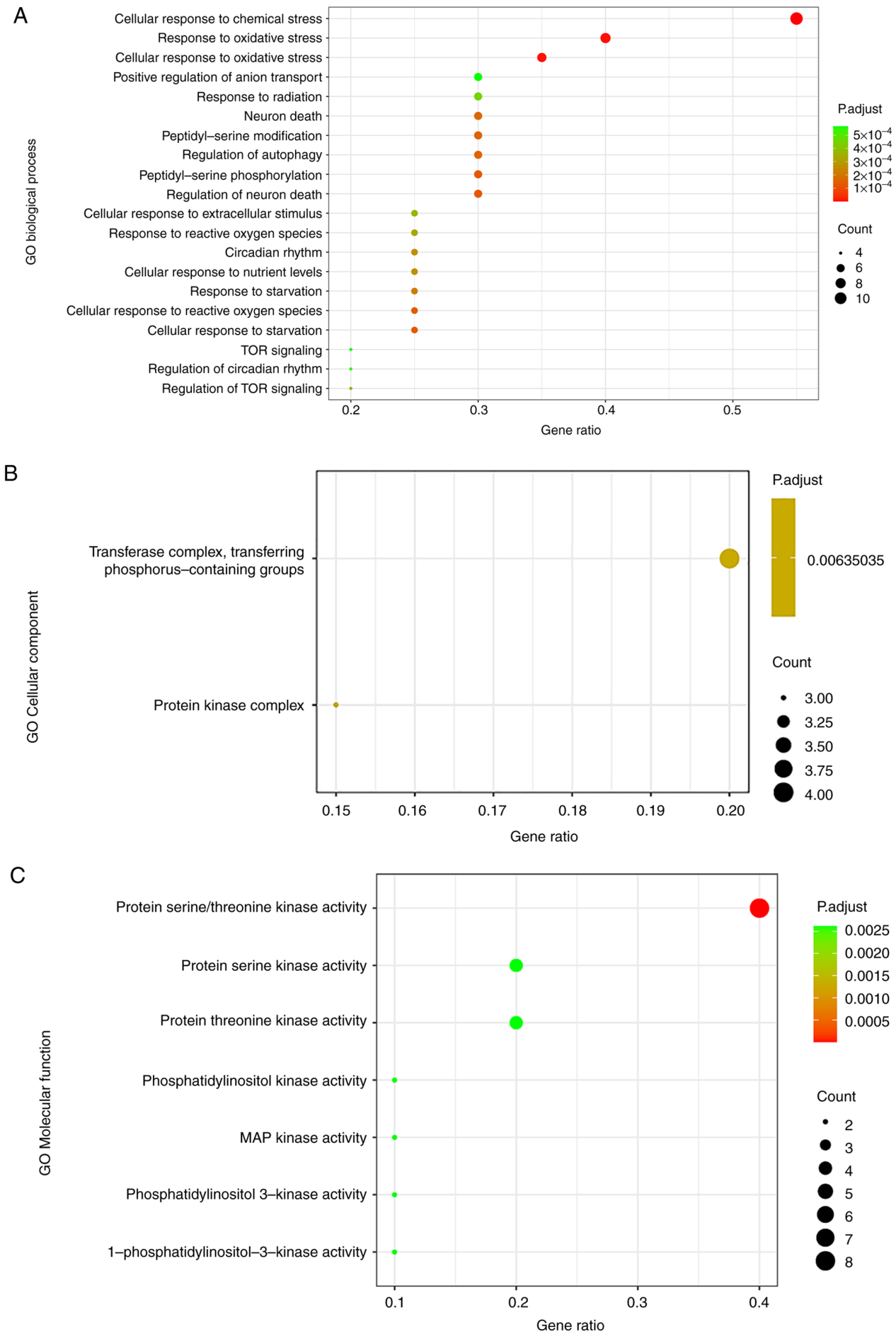

Figure 6. Continued.

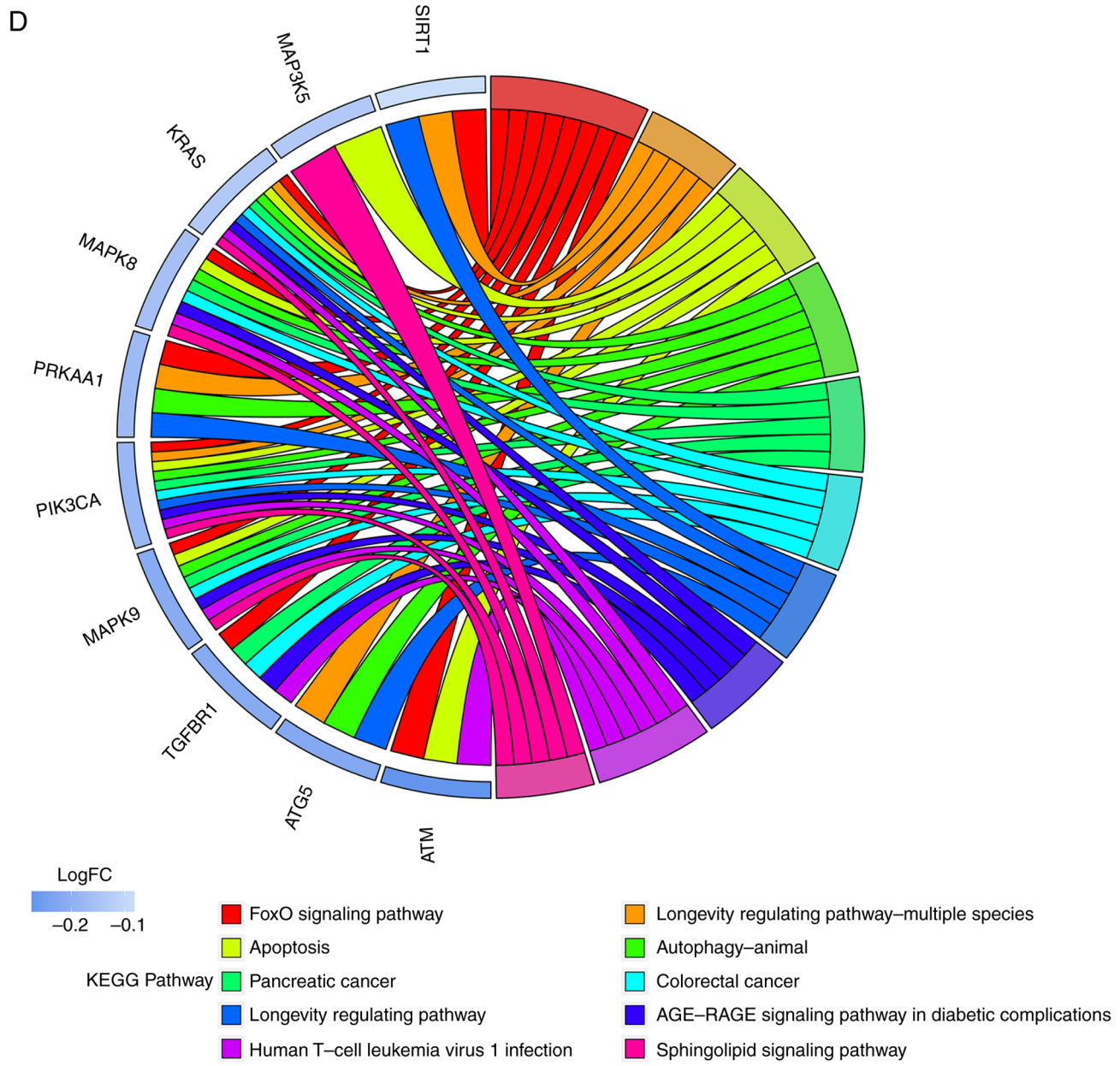

Figure 6. GO and KEGG enrichment analysis of ferroptosis-related genes. GO enrichment analysis of 20 genes for (A) 'biological process', (B) 'cellular component' and (C) 'molecular function'. (D) KEGG enrichment of differentially expressed genes. GO, Gene Ontology; KEGG, Kyoto Encyclopedia of Genes and Genomes; FC, fold change.

using WGCNA, 20 ferroptosis-related genes were identified. Next, the 20 genes were subjected to GO and KEGG enrichment analysis. GO analysis revealed that 'cellular response to chemical stress' and 'response to oxidative stress' were the most significant BPs, while the 20 most influential genes had roles in 'peptidyl-serine' modification, 'protein serine/threonine kinase activity' and 'regulation of TOR signaling'. KEGG analysis indicated that these genes were mainly enriched in 'FoxO signaling pathway', 'Autophagy-animal', 'Apoptosis' and 'Longevity regulating pathway-multiple species'. Furthermore, the recent study has shown that the sources of cellular stress damage can be divided into physicochemical (for example, radiation or toxins) and pathological (for example, hypoxia and infection) (43). Cell stress can cause rapid ROS accumulation, which further aggravates myocardial injury (44). ROS is involved in a variety of coronary diseases that occur under oxidative stress (45). It can affect DNA integrity by inducing mutations, modify protein structure by acting on enzymes and cause lipid peroxidation (46,47). lipid peroxidation is involved in apoptosis, autophagy and ferroptosis, which results in cardiomyocyte dysfunction and death. The underlying mechanism involves excessive ROS attacking the biofilm, which induces a lipid peroxidation chain reaction, and subsequently causes various types of cell death (48). To the best of our knowledge, there are no reports on the FoxO signaling pathway and ferroptosis, and most reports on mammalian target of rapamycin (mTOR) signaling and ferroptosis have focused on tumors. The mTOR and GPX4 signaling pathways mutually regulate autophagy-dependent ferroptosis of pancreatic cancer cells (49). Baba *et al* (50) demonstrated a protective effect of

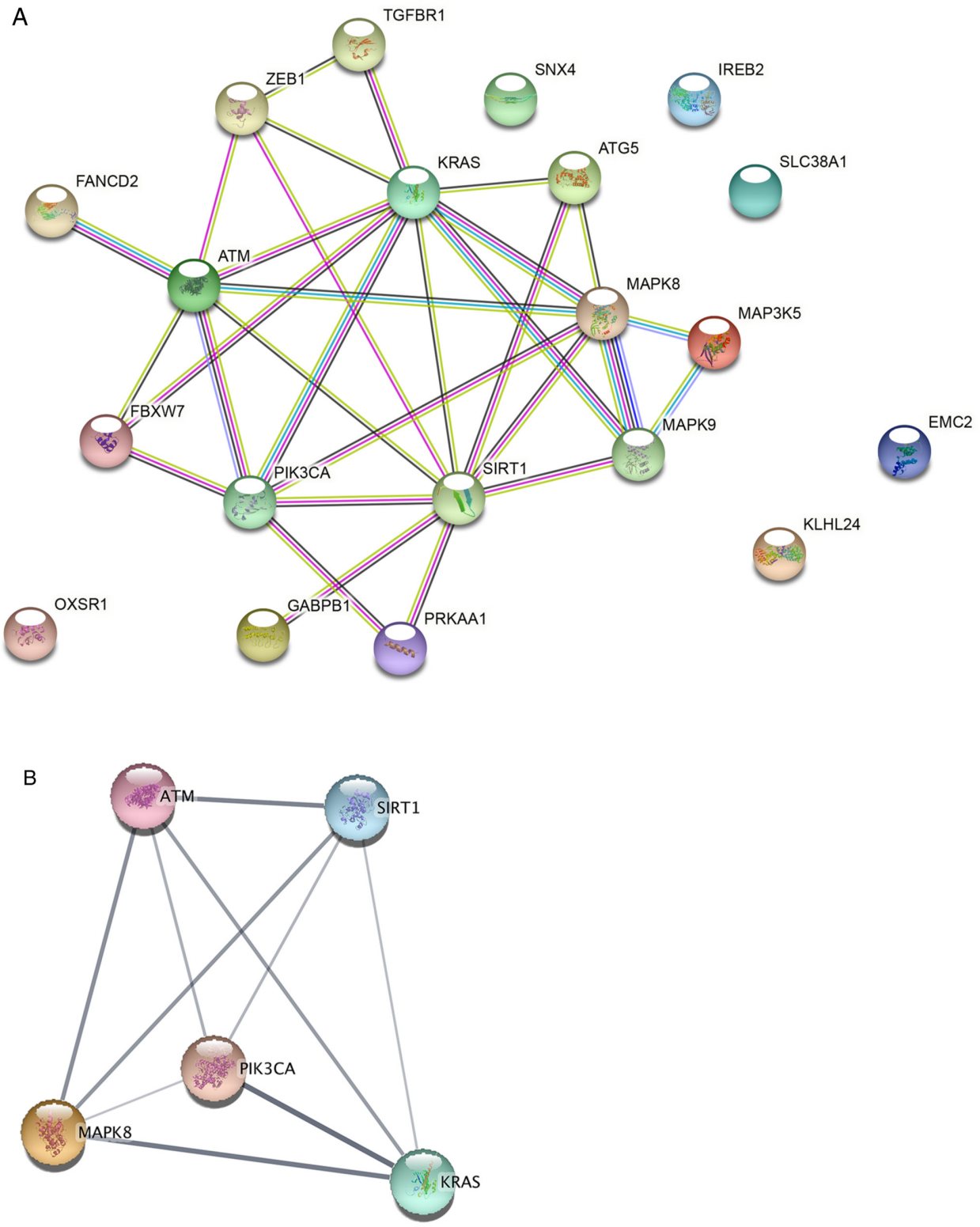

Figure 7. PPI networks. (A) PPI network of 20 genes. (B) PPI subnetwork of hub genes. PPI, protein-protein interaction.

rapamycin-targeted therapy on iron excess and ferroptosis of cardiomyocytes using mTOR-knockout mice and found that it inhibited ROS production. In summary, previous studies on the biological processes that were identified in MI indicate that the 20 key ferroptosis-related genes identified in the present study may affect the occurrence of ferroptosis by regulating ROS production and ultimately MI (51-53).

To further explore the key genes affecting MI, the core modules were screened by PPI network analysis and five hub genes associated with ferroptosis were obtained, namely ATM, PIK3CA, SIRT1, KRAS and MAPK8. Low expression of ATM, PI3KCA and SIRT1 was observed in the GSE141512 validation set. In addition, low expression of the five genes was also observed in serum samples collected from patients with

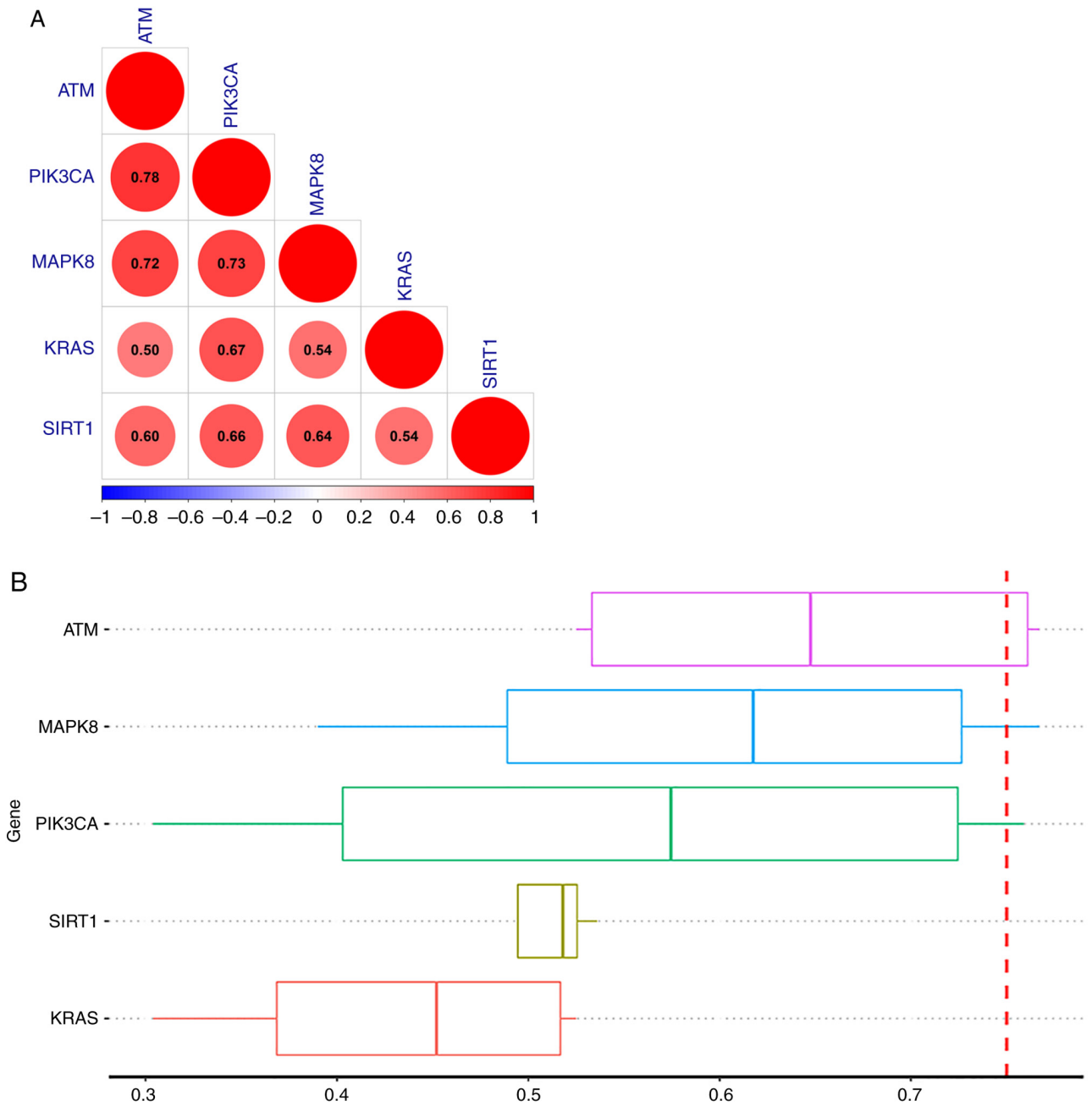

Figure 8. Analysis of interaction effect and functional similarity of hub genes. (A) Expression correlation of hub genes. (B) Function similarity of hub genes.

MI compared with the CCS (control) group. Reduced expression of ATM may protect cells from ferroptosis induced by the GPX4 inhibitor at different concentrations. With respect to the underlying mechanism, ATM inhibition may rescue ferroptosis by increasing the expression of iron regulators involved in iron storage and export. The coordinated changes of these iron regulators during ATM inhibition results in the reduction of labile iron to prevent iron-dependent ferroptosis (54,55). ATM is an important kinase in response to DNA damage and one of its downstream targets, p53, is associated with the regulation of ferroptosis (56). PIK3CA plays an important role in cell growth and survival, and it reduces the inflammatory response following MI through pyruvate dehydrogenase kinase 1/AKT signal transduction (57). The PIK3CA gene regulated by miR-375 is a key gene involved in the MI disease module (58). The expression of SIRT1 decreases gradually after MI and it inhibits ferroptosis-induced cardiomyocyte death through the p53/SLC7A11 axis. The increase in SIRT1 contributes to enhanced cardiomyocyte viability and reduced ferroptosis-induced cell death *in vitro* (13). MAPK8 has been shown to play an important role in the occurrence of recurrent cardiovascular events (59). There are numerous reports on the KRAS gene and tumor-associated diseases (60-62), suggesting that KRAS promotes tumor progression; however, there are few reports on the role of the KRAS gene in MI. Cells undergoing ferroptosis release KRAS (63), but the relationship of MI with the KRAS gene requires further study.

ROC curve analysis can be used to evaluate MI biomarkers. The AUC for ATM, PIK3CA and MAPK8 were all >0.7. Of these, ATM presented the best discrimination performance,

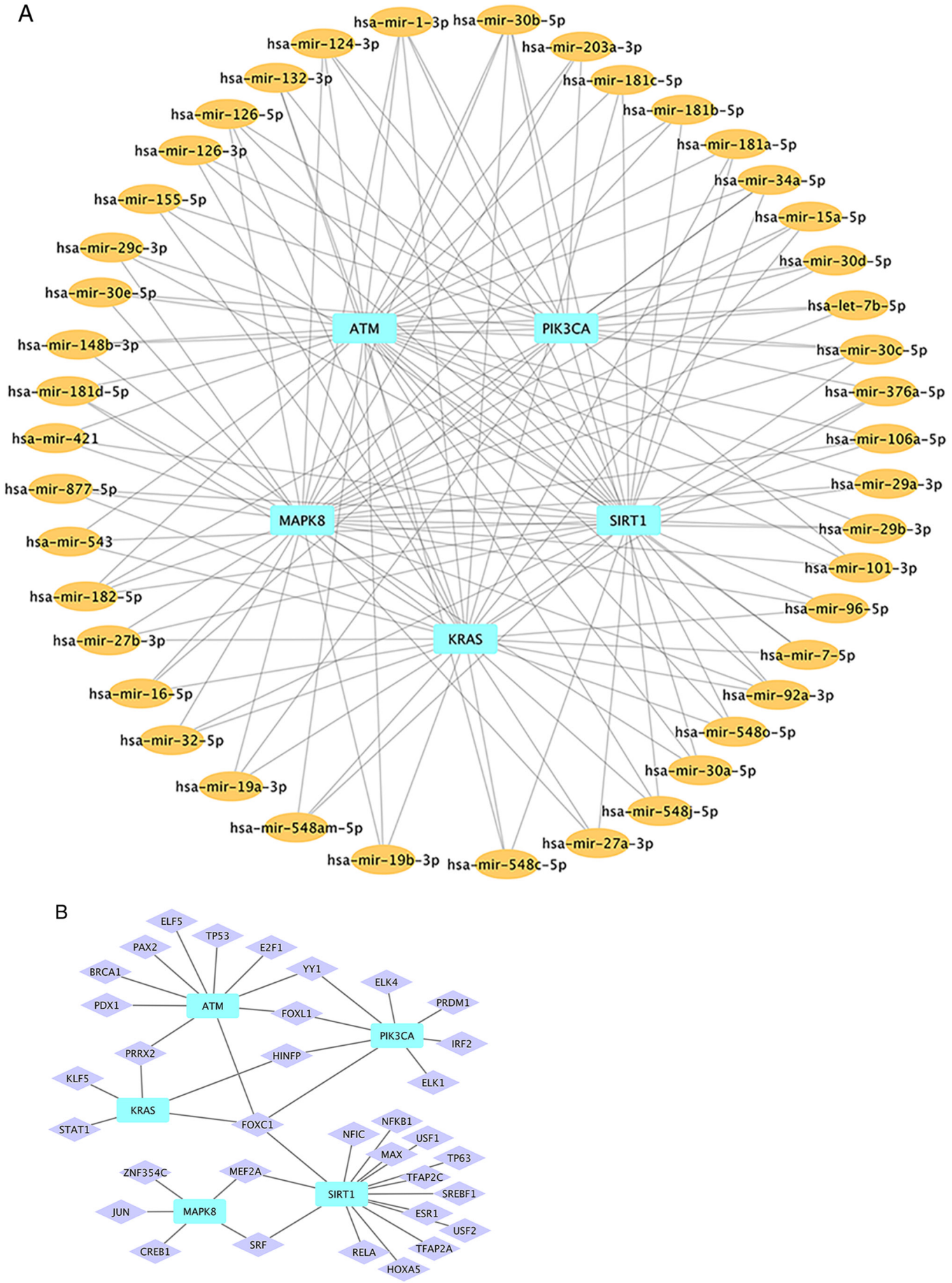

Figure 9. Multi-factor regulation network construction. (A) miRNA regulation network of hub genes. (B) Transcription factor regulation network of hub genes. miRNA/miR, microRNA.

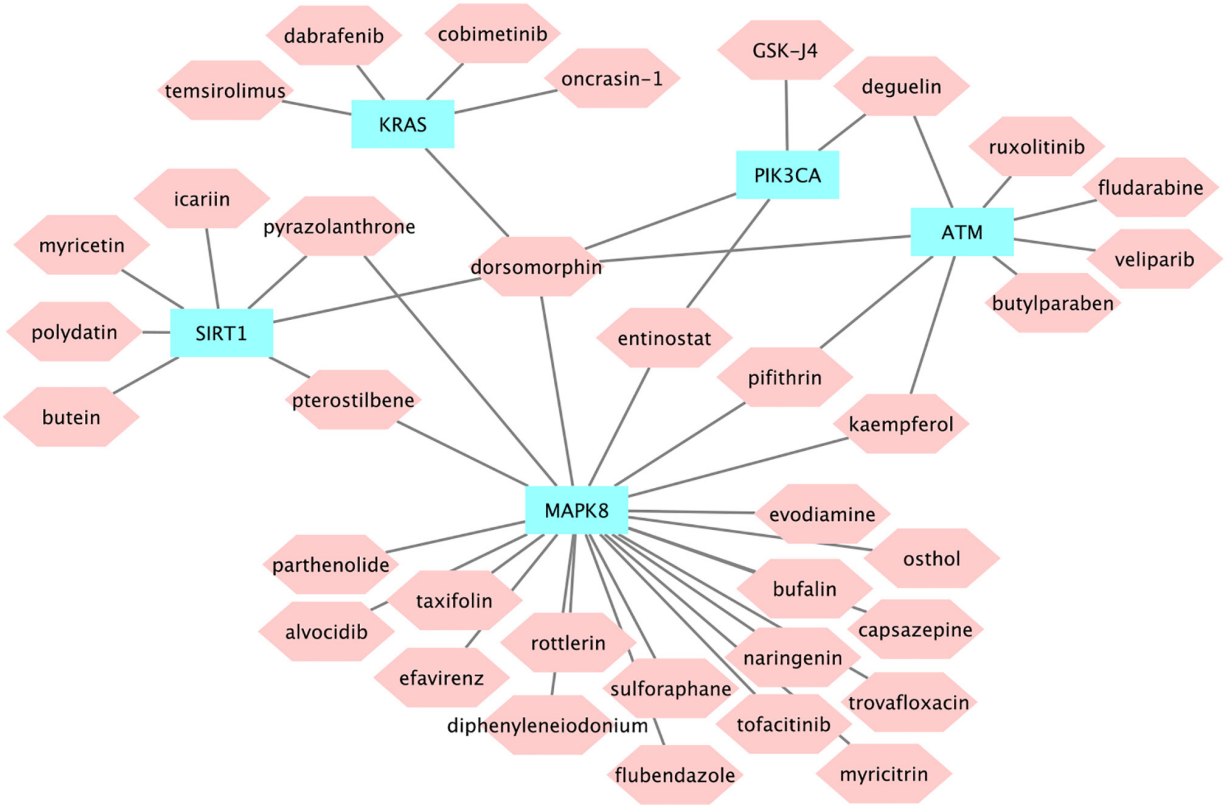

Figure 10. Hub genes and targeted drugs. The light blue rectangle in the figure is the Hub gene, and the light red hexagon is the potential small molecule drug.

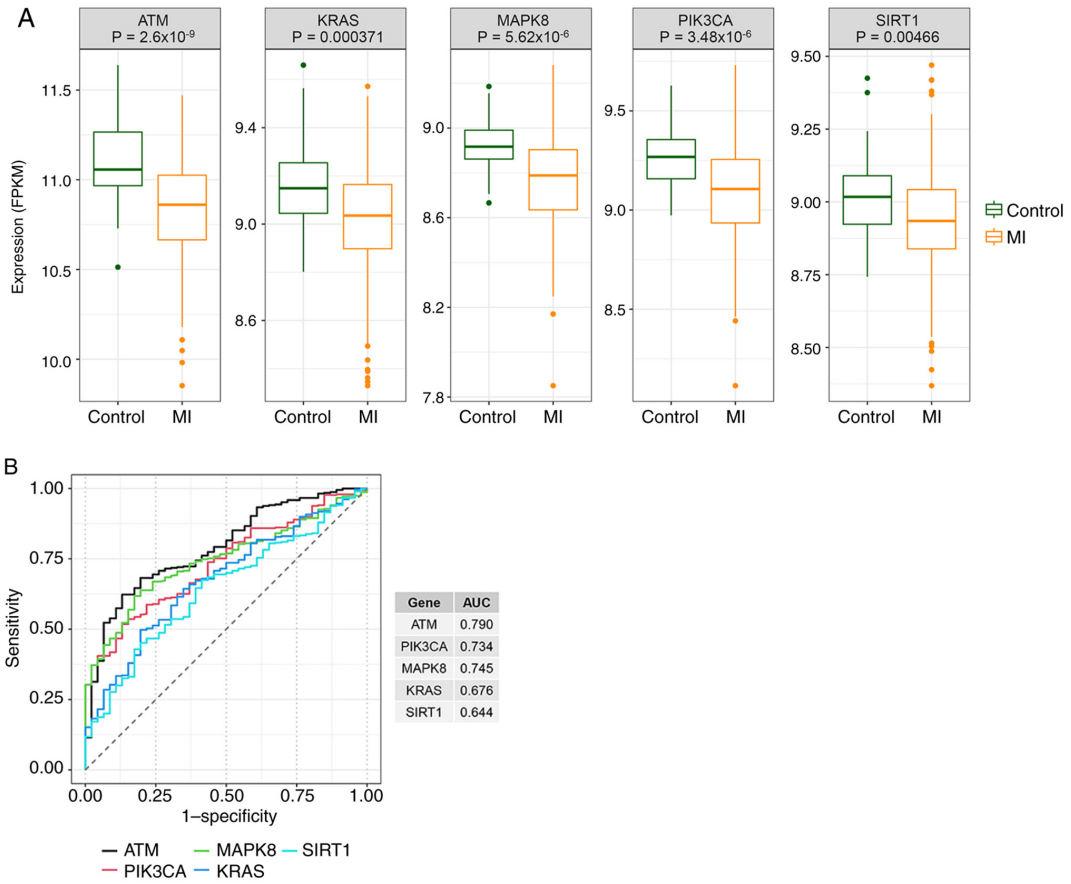

Figure 11. Evaluation of the diagnostic performance of hub genes in GSE59867. (A) Expression of hub genes in control and MI groups. (B) Receiver operating characteristic curves of hub genes for discriminating patients with MI from normal controls. MI, myocardial infarction; FPKM, fragments per kilobase of exon per million mapped fragments; AUC, area under the curve.

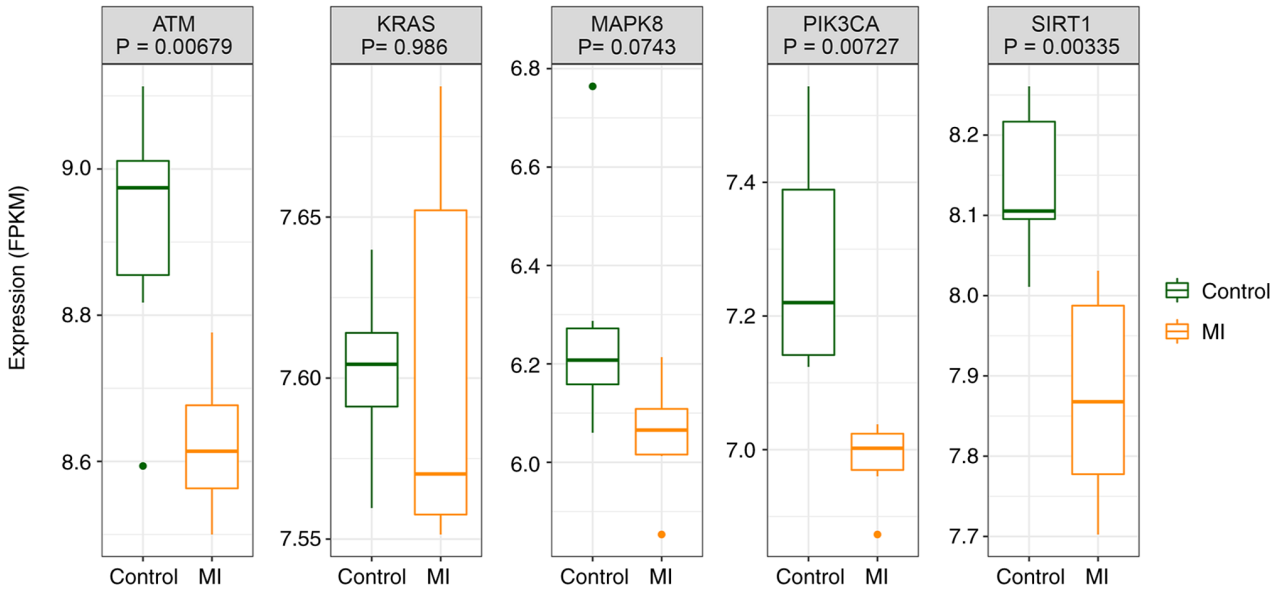

Figure 12. Expression of hub genes in the validation dataset. MI, myocardial infarction.

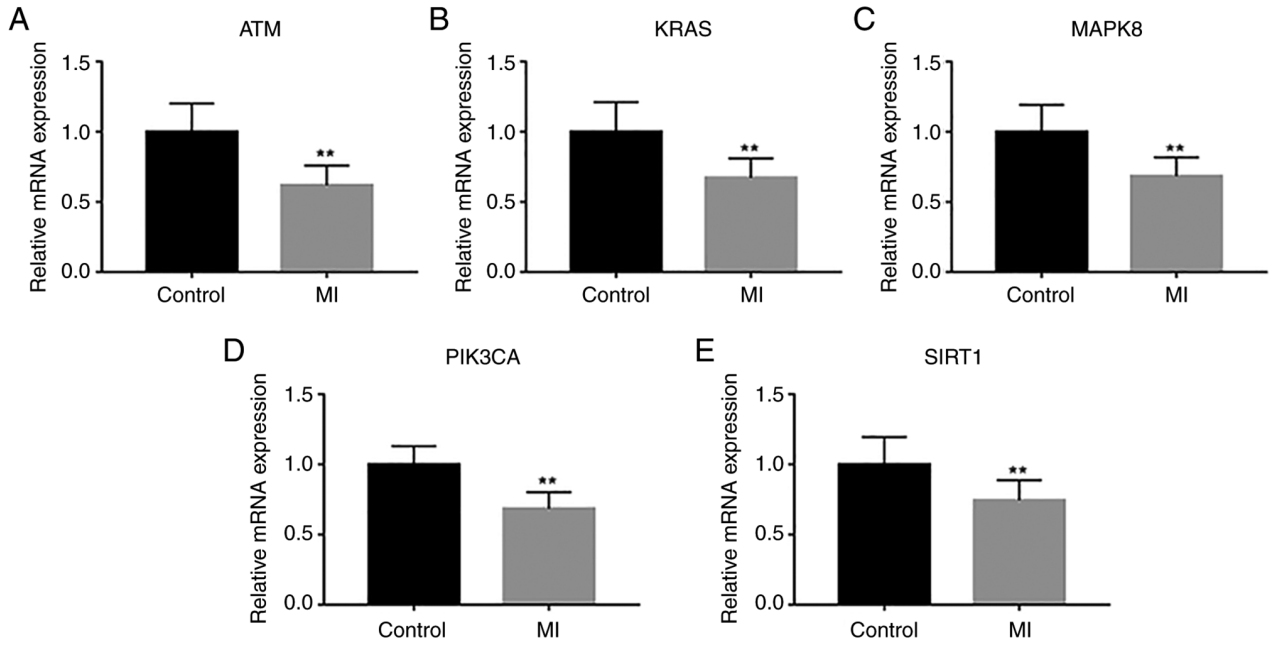

Figure 13. Validation of hub genes in patients with MI. Graphs showing the relative mRNA expression levels in controls compared with patients with MI for (A) ATM, (B) KRAS, (C) MAPK8, (D) PIK3CA and (E) SIRT1. **P<0.01. MI, myocardial infarction.

with an AUC of 0.790. TF-target and miRNA-target networks relevant to the hub genes were constructed, which highlighted 43 miRNAs and 34 TFs. Finally, the potential small-molecule drugs that could reverse this disease were investigated using the CMap database, which revealed 36 potential small-molecule drugs. Among them, dorsomorphin is a small-molecule drug that can act on all five hub genes. Dorsomorphin is a selective inhibitor of AMP-activated protein kinase (64), which has not been well-studied in MI. Therefore, its role should be the subject of future studies.

The present study had the following strengths: i) The GSE59867 dataset included data from 390 MI samples and 46 healthy individuals, with a large sample size and high reliability of results; ii) verification was done twice using the GSE141512 dataset and by collecting and evaluating patient blood samples; and iii) for the first time, bioinformatics analysis was used to identify the hub genes of ferroptosis and MI. However, the identified marker genes and pathways require further verification to provide conclusive evidence for targeted therapy; if the protein expression of these genes can be further analyzed, more evidence will be available to determine the effect of each gene on ferroptosis and MI.

In conclusion, the current study identified five putative genes relevant to ferroptosis and numerous genes associated with MI, which provides a basis for exploring the regulatory and intervening mechanisms of MI.

Table II. Demographics, clinical features, medication history and laboratory data of all participants.

Variable	Control (n=5)	MI (n=5)	P-value
Demographic features			
Age, years[a]	59.20±10.66	58.00±10.32	0.861
Male sex[c]	3 (60.00)	4 (80.00)	>0.999
Cardiovascular risk factors			
Hypertension[c]	2 (40.00)	3 (60.00)	>0.999
Dyslipidemia[c]	2 (40.00)	4 (80.00)	0.524
Diabetes mellitus[c]	2 (40.00)	3 (60.00)	>0.999
Current smoking[c]	3 (60.00)	4 (80.00)	>0.999
Vital signs on admission			
SBP, mmHg[b]	131.00 (129.00-134.00)	134.00 (131.00-152.00)	0.293
DBP, mmHg[a]	78.60±11.39	85.60±16.04	0.449
Heart rate, beats/min[a]	80.40±20.03	76.80±13.77	0.749
Echocardiographic findings			
LVEF, %[a]	57.40±6.35	46.80±8.64	0.058
Laboratory findings			
hs-cTnI, ng/ml[b]	0.08 (0.05-0.10)	30.00 (24.50-30.00)	0.011
CKMB, U/l[a]	2.48±0.88	11.66±3.48	0.003
NT-pro-BNP, pg/ml[b]	101.00 (86.00-201.00)	1,106.0 (151.00-3,245.00)	0.296
TC, mmol/l[a]	3.86±0.70	4.67±0.87	0.142
TG, mmol/l[a]	1.15±0.11	1.04±0.34	0.517
LDL-C, mmol/l[a]	2.39±0.44	3.41±0.79	0.036
HDL-C, mmol/l[a]	0.95±0.06	0.96±0.09	0.869
Medication history			
Aspirin[c]	1 (20.00)	2 (40.00)	>0.999
Clopidogrel[c]	1 (20.00)	1 (20.00)	>0.999
Statin[c]	1 (20.00)	3 (60.00)	0.524
ACEI/ARB[c]	2 (40.00)	2 (40.00)	>0.999
β blocker[c]	2 (40.00)	2 (40.00)	>0.999
CCB[c]	1 (20.00)	2 (40.00)	>0.999

[a]Result is expressed as the mean ± standard deviation and the P-value has been obtained using independent t-test. [b]Result is expressed as the median (quartile 1-quartile 3) and the P-value has been obtained using Mann-Whitney U test. [c]Result is expressed as the number of cases (composition ratio, %), and the P-value has been obtained using χ^2 test or Fisher's exact test if the theoretical frequency of the variable was too small. MI, myocardial infarction; SBP, systolic blood pressure; DBP, diastolic blood pressure; LVEF, left ventricular ejection fraction; hs-cTnI, high-sensitivity cardiac troponin I; CKMB, creatine kinase-MB; NT-pro-BNP, n-terminal pro-B-type natriuretic peptide; TC, total cholesterol; TG, triglyceride; LDL-C, low-density lipoprotein-cholesterol; HDL-C, high-density lipoprotein-cholesterol; ACEI, angiotensin converting enzyme inhibitors; ARB, angiotensin II receptor blockers; CCB, calcium channel blockers.

Acknowledgements

Not applicable.

Funding

Funding for the present study was obtained from the Shandong Province Famous and Old Traditional Chinese Medicine Expert Inheritance Studio Construction Project (grant no. 201992), the Shandong Traditional Chinese Medicine Science and Technology Project (grant nos. 2020Q010 and 2021M180) and the Natural Science Foundation of Shandong Province (grant no. ZR2021LZY038).

Availability of data and materials

The datasets used and/or analyzed during the current study are available from the corresponding author on reasonable request.

Authors' contributions

YHJ, WZW and YTX confirm the authenticity of all the raw data. YHJ, WZW and YTX were responsible for the conceptualization, methodology and design of the research, as well as writing and preparing the original draft. SYW and ZW were responsible for the bioinformatic data collection and analysis. JZ, YL, LZ and CL were responsible for the experimental data acquisition and analysis. JZ and YL were responsible

for the software validation and result interpretation. CL was responsible for the figure preparation. All authors have read and approved the final manuscript.

Ethics approval and consent to participate

The present study was approved by the Ethics Committee of Dezhou Municipal Hospital (Dezhou, China; approval no. 2022-L-06; January 17, 2022) and complied with The Declaration of Helsinki. Written informed consent was obtained from all subjects.

Patient consent for publication

Not applicable.

Competing interests

The authors declare that they have no competing interests.

References

1. Camacho X, Nedkoff L, Wright FL, Nghiem N, Buajitti E, Goldacre R, Rosella LC, Seminog O, Tan EJ, Hayes A, *et al*: Relative contribution of trends in myocardial infarction event rates and case fatality to declines in mortality: An international comparative study of 1·95 million events in 80·4 million people in four countries. Lancet Public Health 7: e229-e239, 2022.
2. Thygesen K, Alpert JS, Jaffe AS, Simoons ML, Chaitman BR, White HD, Thygesen K, Alpert JS, White HD, Jaffe AS, *et al*: Third universal definition of myocardial infarction. J Am Coll Cardiol 60: 1581-1598, 2012.
3. Thygesen K, Alpert JS, Jaffe AS, Chaitman BR, Bax JJ, Morrow DA and White HD: Fourth universal definition of myocardial infarction (2018). J Am Coll Cardiol 72: 2231-2264, 2018.
4. Collet JP, Thiele H, Barbato E, Barthélémy O, Bauersachs J, Bhatt DL, Dendale P, Dorobantu M, Edvardsen T, Folliguet T, *et al*: 2020 ESC guidelines for the management of acute coronary syndromes in patients presenting without persistent ST-segment elevation. Eur Heart J 42: 1289-1367, 2021.
5. Ibanez B, James S, Agewall S, Antunes MJ, Bucciarelli-Ducci C, Bueno H, Caforio A, Crea F, Goudevenos JA, Halvorsen S, *et al*: 2017 ESC guidelines for the management of acute myocardial infarction in patients presenting with ST-segment elevation: The task force for the management of acute myocardial infarction in patients presenting with ST-segment elevation of the European society of cardiology (ESC). Eur Heart J 39: 119-177, 2018.
6. Spione F, Arevalos V, Gabani R, Sabaté M and Brugaletta S: Coronary microvascular angina: A state-of-the-art review. Front Cardiovasc Med 9: 800918, 2022.
7. Jiang X, Stockwell BR and Conrad M: Ferroptosis: Mechanisms, biology and role in disease. Nat Rev Mol Cell Biol 22: 266-282, 2021.
8. Wang J, Liu Y, Wang Y and Sun L: The cross-link between ferroptosis and kidney diseases. Oxid Med Cell Longev 2021: 6654887, 2021.
9. Chen C, Wang D, Yu Y, Zhao T, Min N, Wu Y, Kang L, Zhao Y, Du L, Zhang M, *et al*: Legumain promotes tubular ferroptosis by facilitating chaperone-mediated autophagy of GPX4 in AKI. Cell Death Dis 12: 65, 2021.
10. Zhao L, Zhou X, Xie F, Zhang L, Yan H, Huang J, Zhang C, Zhou F, Chen J and Zhang L: Ferroptosis in cancer and cancer immunotherapy. Cancer Commun (Lond) 42: 88-116, 2022.
11. Wu X, Li Y, Zhang S and Zhou X: Ferroptosis as a novel therapeutic target for cardiovascular disease. Theranostics 11: 3052-3059, 2021.
12. Li W, Li W, Leng Y, Xiong Y and Xia Z: Ferroptosis is involved in diabetes myocardial ischemia/reperfusion injury through endoplasmic reticulum stress. DNA Cell Biol 39: 210-225, 2020.
13. Ma S, Sun L, Wu W, Wu J, Sun Z and Ren J: USP22 protects against myocardial ischemia-reperfusion injury via the SIRT1-p53/SLC7A11-dependent inhibition of ferroptosis-induced cardiomyocyte death. Front Physiol 11: 551318, 2020.
14. Jelinek A, Heyder L, Daude M, Plessner M, Krippner S, Grosse R, Diederich WE and Culmsee C: Mitochondrial rescue prevents glutathione peroxidase-dependent ferroptosis. Free Radic Biol Med 117: 45-57, 2018.
15. Chen HY, Xiao ZZ, Ling X, Xu RN, Zhu P and Zheng SY: ELAVL1 is transcriptionally activated by FOXC1 and promotes ferroptosis in myocardial ischemia/reperfusion injury by regulating autophagy. Mol Med 27: 14, 2021.
16. Fang X, Wang H, Han D, Xie E, Yang X, Wei J, Gu S, Gao F, Zhu N, Yin X, *et al*: Ferroptosis as a target for protection against cardiomyopathy. Proc Natl Acad Sci USA 116: 2672-2680, 2019.
17. Fan Z, Cai L, Wang S, Wang J and Chen B: Baicalin prevents myocardial ischemia/reperfusion injury through inhibiting ACSL4 mediated ferroptosis. Front Pharmacol 12: 628988, 2021.
18. Eling N, Reuter L, Hazin J, Hamacher-Brady A and Brady NR: Identification of artesunate as a specific activator of ferroptosis in pancreatic cancer cells. Oncoscience 2: 517-532, 2015.
19. Linkermann A, Skouta R, Himmerkus N, Mulay SR, Dewitz C, De Zen F, Prokai A, Zuchtriegel G, Krombach F, Welz PS, *et al*: Synchronized renal tubular cell death involves ferroptosis. Proc Natl Acad Sci U S A 111: 16836-16841, 2014.
20. Maciejak A, Kiliszek M, Michalak M, Tulacz D, Opolski G, Matlak K, Dobrzycki S, Segiet A, Gora M and Burzynska B: Gene expression profiling reveals potential prognostic biomarkers associated with the progression of heart failure. Genome Med 7: 26, 2015.
21. Osmak G, Baulina N, Koshkin P and Favorova O: Collapsing the list of myocardial infarction-related differentially expressed genes into a diagnostic signature. J Transl Med 18: 231, 2020.
22. Barrett T, Wilhite SE, Ledoux P, Evangelista C, Kim IF, Tomashevsky M, Marshall KA, Phillippy KH, Sherman PM, Holko M, *et al*: NCBI GEO: Archive for functional genomics data sets-update. Nucleic Acids Res 41: D991-D995, 2013.
23. Tian Q, Zhou Y, Zhu L, Gao H and Yang J: Development and validation of a ferroptosis-related gene signature for overall survival prediction in lung adenocarcinoma. Front Cell Dev Biol 9: 684259, 2021.
24. Chan B: Data analysis using R programming. Adv Exp Med Biol 1082: 47-122, 2018.
25. Love MI, Huber W and Anders S: Moderated estimation of fold change and dispersion for RNA-seq data with DESeq2. Genome Biol 15: 550, 2014.
26. Qian L, Xia Z, Zhang M, Han Q, Hu D, Qi S, Xing D, Chen Y and Zhao X: Integrated bioinformatics-based identification of potential diagnostic biomarkers associated with diabetic foot ulcer development. J Diabetes Res 2021: 5445349, 2021.
27. Langfelder P and Horvath S: WGCNA: An R package for weighted correlation network analysis. BMC Bioinformatics 9: 559, 2008.
28. The Gene Ontology Consortium: Expansion of the gene ontology knowledgebase and resources. Nucleic Acids Res 45: D331-D338, 2017.
29. Kanehisa M and Goto S: KEGG: Kyoto encyclopedia of genes and genomes. Nucleic Acids Res 28: 27-30, 2000.
30. Szklarczyk D, Franceschini A, Wyder S, Forslund K, Heller D, Huerta-Cepas J, Simonovic M, Roth A, Santos A, Tsafou KP, *et al*: STRING v10: Protein-protein interaction networks, integrated over the tree of life. Nucleic Acids Res 43: D447-D452, 2015.
31. Shannon P, Markiel A, Ozier O, Baliga NS, Wang JT, Ramage D, Amin N, Schwikowski B and Ideker T: Cytoscape: A software environment for integrated models of biomolecular interaction networks. Genome Res 13: 2498-2504, 2003.
32. Robin X, Turck N, Hainard A, Tiberti N, Lisacek F, Sanchez JC and Müller M: pROC: An open-source package for R and S+ to analyze and compare ROC curves. BMC Bioinformatics 12: 77, 2011.
33. Zhang Y, Shen B, Zhuge L and Xie Y: Identification of differentially expressed genes between the colon and ileum of patients with inflammatory bowel disease by gene co-expression analysis. J Int Med Res 48: 300060519887268, 2020.
34. Han Y, Yu G, Sarioglu H, Caballero-Martinez A, Schlott F, Ueffing M, Haase H, Peschel C and Krackhardt AM: Proteomic investigation of the interactome of FMNL1 in hematopoietic cells unveils a role in calcium-dependent membrane plasticity. J Proteomics 78: 72-82, 2013.
35. Davis AP, Grondin CJ, Johnson RJ, Sciaky D, Wiegers J, Wiegers TC and Mattingly CJ: Comparative toxicogenomics database (CTD): Update 2021. Nucleic Acids Res 49: D1138-D1143, 2021.

36. Chang L, Zhou G, Soufan O and Xia J: miRNet 2.0: Network-based visual analytics for miRNA functional analysis and systems biology. Nucleic Acids Res 48: W244-W251, 2020.
37. Diamond GA: A clinically relevant classification of chest discomfort. J Am Coll Cardiol 1: 574-575, 1983.
38. Montalescot G, Sechtem U, Achenbach S, Andreotti F, Arden C, Budaj A, Bugiardini R, Crea F, Cuisset T, Di Mario C, *et al*: 2013 ESC guidelines on the management of stable coronary artery disease: The task force on the management of stable coronary artery disease of the European society of cardiology. Eur Heart J 34: 2949-3003, 2013.
39. Fihn SD, Gardin JM, Abrams J, Berra K, Blankenship JC, Dallas AP, Douglas PS, Foody JM, Gerber TC, Hinderliter AL, *et al*: 2012 ACCF/AHA/ACP/AATS/PCNA/SCAI/STS guideline for the diagnosis and management of patients with stable ischemic heart disease: A report of the American college of cardiology foundation/American heart association task force on practice guidelines, and the American college of physicians, American association for thoracic surgery, preventive cardiovascular nurses association, society for cardiovascular angiography and interventions, and society of thoracic surgeons. Circulation 126: e354-e471, 2012.
40. Livak KJ and Schmittgen TD: Analysis of relative gene expression data using real-time quantitative PCR and the 2(-Delta Delta C(T)) method. Methods 25: 402-408, 2001.
41. Lamb J, Crawford ED, Peck D, Modell JW, Blat IC, Wrobel MJ, Lerner J, Brunet JP, Subramanian A, Ross KN, *et al*: The connectivity map: Using gene-expression signatures to connect small molecules, genes, and disease. Science 313: 1929-1935, 2006.
42. Wen W, Wu P, Zhang Y, Chen Z, Sun J and Chen H: Comprehensive analysis of NAFLD and the therapeutic target identified. Front Cell Dev Biol 9: 704704, 2021.
43. Contessotto P and Pandit A: Therapies to prevent post-infarction remodelling: From repair to regeneration. Biomaterials 275: 120906, 2021.
44. Zhou T, Chuang CC and Zuo L: Molecular characterization of reactive oxygen species in myocardial ischemia-reperfusion injury. Biomed Res Int 2015: 864946, 2015.
45. Khosravi M, Poursaleh A, Ghasempour G, Farhad S and Najafi M: The effects of oxidative stress on the development of atherosclerosis. Biol Chem 400: 711-732, 2019.
46. Ravingerová T, Kindernay L, Barteková M, Ferko M, Adameová A, Zohdi V, Bernátová I, Ferenczyová K and Lazou A: The molecular mechanisms of iron metabolism and its role in cardiac dysfunction and cardioprotection. Int J Mol Sci 21: 7889, 2020.
47. Kura B, Bacova BS, Kalocayova B, Sykora M and Slezak J: Oxidative stress-responsive MicroRNAs in heart injury. Int J Mol Sci 21: 358, 2020.
48. Su LJ, Zhang JH, Gomez H, Murugan R, Hong X, Xu D, Jiang F and Peng ZY: Reactive oxygen species-induced lipid peroxidation in apoptosis, autophagy, and ferroptosis. Oxid Med Cell Longev 2019: 5080843, 2019.
49. Liu Y, Wang Y, Liu J, Kang R and Tang D: Interplay between MTOR and GPX4 signaling modulates autophagy-dependent ferroptotic cancer cell death. Cancer Gene Ther 28: 55-63, 2021.
50. Baba Y, Higa JK, Shimada BK, Horiuchi KM, Suhara T, Kobayashi M, Woo JD, Aoyagi H, Marh KS, Kitaoka H and Matsui T: Protective effects of the mechanistic target of rapamycin against excess iron and ferroptosis in cardiomyocytes. Am J Physiol Heart Circ Physiol 314: H659-H668, 2018.
51. Shen Y, Chen X, Chi C, Wang H, Xue J, Su D, Wang H, Li M, Liu B and Dong Q: Smooth muscle cell-specific knockout of FBW7 exacerbates intracranial atherosclerotic stenosis. Neurobiol Dis 132: 104584, 2019.
52. Ji Y, Luo J, Zeng J, Fang Y, Liu R, Luan F and Zeng N: Xiaoyao pills ameliorate depression-like behaviors and oxidative stress induced by olfactory bulbectomy in rats via the activation of the PIK3CA-AKT1-NFE2L2/BDNF signaling pathway. Front Pharmacol 12: 643456, 2021.
53. Park S, Shin J, Bae J, Han D, Park SR, Shin J, Lee SK and Park HW: SIRT1 alleviates LPS-induced IL-1β production by suppressing NLRP3 inflammasome activation and ROS production in trophoblasts. Cells 9: 728, 2020.
54. Chen PH, Wu J, Ding CC, Lin CC, Pan S, Bossa N, Xu Y, Yang WH, Mathey-Prevot B and Chi JT: Kinome screen of ferroptosis reveals a novel role of ATM in regulating iron metabolism. Cell Death Differ 27: 1008-1022, 2020.
55. Shimada K, Skouta R, Kaplan A, Yang WS, Hayano M, Dixon SJ, Brown LM, Valenzuela CA, Wolpaw AJ and Stockwell BR: Global survey of cell death mechanisms reveals metabolic regulation of ferroptosis. Nat Chem Biol 12: 497-503, 2016.
56. Smith J, Tho LM, Xu N and Gillespie DA: The ATM-Chk2 and ATR-Chk1 pathways in DNA damage signaling and cancer. Adv Cancer Res 108: 73-112, 2010.
57. Garikipati V, Verma SK, Jolardarashi D, Cheng Z, Ibetti J, Cimini M, Tang Y, Khan M, Yue Y, Benedict C, *et al*: Therapeutic inhibition of miR-375 attenuates post-myocardial infarction inflammatory response and left ventricular dysfunction via PDK-1-AKT signalling axis. Cardiovasc Res 113: 938-949, 2017.
58. Baulina N, Osmak G, Kiselev I, Matveeva N, Kukava N, Shakhnovich R, Kulakova O and Favorova O: NGS-identified circulating miR-375 as a potential regulating component of myocardial infarction associated network. J Mol Cell Cardiol 121: 173-179, 2018.
59. Liao J, Chen Z, He Q, Liu Y and Wang J: Differential gene expression analysis and network construction of recurrent cardiovascular events. Mol Med Rep 13: 1746-1764, 2016.
60. Tang D, Kroemer G and Kang R: Oncogenic KRAS blockade therapy: Renewed enthusiasm and persistent challenges. Mol Cancer 20: 128, 2021.
61. Wang X, Wang J, Chen F, Zhong Z and Qi L: Detection of K-ras gene mutations in feces by magnetic nanoprobe in patients with pancreatic cancer: A preliminary study. Exp Ther Med 15: 527-531, 2018.
62. Huang L, Guo Z, Wang F and Fu L: KRAS mutation: From undruggable to druggable in cancer. Signal Transduct Target Ther 6: 386, 2021.
63. Dai E, Han L, Liu J, Xie Y, Kroemer G, Klionsky DJ, Zeh HJ, Kang R, Wang J and Tang D: Autophagy-dependent ferroptosis drives tumor-associated macrophage polarization via release and uptake of oncogenic KRAS protein. Autophagy 16: 2069-2083, 2020.
64. Jaschke N, Kleymann A, Hofbauer LC, Göbel A and Rachner TD: Dorsomorphin: A novel inhibitor of Dickkopf-1 in breast cancer. Biochem Biophys Res Commun 524: 360-365, 2020.